Eleventh Quarterly Progress Report

N01-DC-9-2107

The Neurophysiological Effects of Simulated Auditory Prosthesis Stimulation

H. Mino, J.T. Rubinstein, C.A. Miller, P.J. Abbas

Department of Otolaryngology - Head and Neck Surgery
Department of Speech Pathology and Audiology
Department of Physiology and Biophysics
Department of Biomedical Engineering
University of Iowa
Iowa City, IA 52242

July 31, 2002

Contents

1   Introduction

The purpose of this contract is to explore issues involving the transfer of information from implantable auditory prostheses to the central nervous system. Our investigation is being pursued along multiple tracks and include the use of animal experiments and computer model simulations to:

1. Characterize the fundamental spatial and temporal properties of intracochlear stimulation of the auditory nerve.

2. Evaluate the use of novel stimuli and electrode arrays.

3. Evaluate proposed enhancements in animal models of partial degeneration of the auditory nerve.

In this eleventh quarterly progress report (QPR), we focus on the first of these three aims, reporting on computer simulations characterizing how refractory properties can influence the variation of spike initiations in an auditory nerve fiber (ANF) model with nodes of Ranvier containing stochastic sodium and potassium channels.

2   Summary of activities in this quarter

In our eleventh quarter (1 April - 30 June, 2002), the following activities related to this contract were completed:

1. A major area of focus was the collection of the electrically evoked compound action potential (ECAP) in response to pulse-train stimulation. Six acute experiments with guinea pigs were conducted to characterize response adaptation over the course of the pulse trains. These results will be presented in a future progress report.

2. We prepared and submitted (for peer review) a manuscript that detailed our investigations of the influence of electrode configuration (i.e., monopolar vs. bipolar) on the electrically evoked response of the feline auditory nerve. Preliminary findings were reported in QPR 9.

3. We began a new series of experiments investigating the influence of the recording electrode position on various characteristics of the electrically evoked compound action potential. Clinical techniques of recordings the ECAP employ intracochlear recording sites, while our animal

research protocols have employed electrodes positioned on the surgically exposed nerve. We intend to use a within-animal comparisons of both intracochlear and extracochlear recording sites to determine the effect of electrode position on ECAP morphology, latency, and growth. To date, we have conducted one experiment using a feline-scaled banded Nucleus electrode array.

4. We performed an acute experiment with a Michigan NASA 1 thin-film electrode to characterize the spatial selectivity of this recording probe. Previously, we have used the PSU 4/5 family of electrodes (or custom variants) to investigate spatial response areas within the nerve trunk using acoustic tone-burst stimuli. The NASA 1 design featured a single shank with eight electrodes with surface areas approximately one-sixth that of the PSU 4/5 family. We again used tone-burst stimuli to assess spatial specificity of the recording electrodes in both monopolar and differential (bipolar) recording modes. Our results indicate that, as in the case of the PSU 4/5 experiments, some spatial selectivity is evident in the recordings. However, the degree of selectivity was comparable to that produced by the PSU 4/5 electrodes and, hence, not sufficient for our intended purposes. We suspect that, in the case of the auditory nerve, the relatively small neural targets necessitate small electrode pad sizes. In conjunction with the Michigan group, we hope to further explore the use of electrode designs with favorable characteristics for intraneural recordings.

3   How can refractoriness influence spike initiations?

3.1   Introduction

Computer simulation studies have played an important role in investigating the influence of various parameters on nerve fiber excitation. An ANF model with nodes of Ranvier containing stochastic sodium and potassium channels has been developed in order to realize spike time fluctuations observed in cat single-fiber experiments. Some fundamental properties of the ANF model have been reported in the seventh QPR with regards to the temporal variation of spike times in response to a single monophasic stimulus pulse as the electrode-to-fiber distance varies (Mino, et al., 2001). However, it is still unclear how refractory properties affect the spike response properties beyond the single stimulus pulse situation discussed in the seventh

QPR. Refractory properties could influence the spatio-temporal variation of spike initiations in response to a probe pulse under a double-pulse (masker-probe) stimulus strategy in which the masker pulse evokes action potentials for each stimulus presentation (FE=1.0 for masker pulse). The knowledge of how spikes are initiated during refractory periods might contribute to understanding how electrically stimulated ANFs can be desyncronized with a high-rate conditioning stimulus (Rubinstein, et al., 1999; Litvak, 2002; Runge-Samuelson, 2002; Hong, et al., 2002). Although fundamental properties of refractoriness have been investigated in physiologic experiments (Li and Young, 1993; Miller, et al, 2001), the analysis of spike initiations can be done only by computer simulations. In this eleventh QPR, we investigate the effects of masker-probe intervals (MPIs) as well as the electrode-to-fiber distance on the spatial and/or temporal properties of spike initiations, using our ANF model.

3.2   Methods

Auditory nerve fibers were represented by a multi-compartment cable model with 50 nodal sections as described in the seventh QPR (Mino et al., 2001). The 50 nodes of Ranvier consisted of stochastic ion channels, 180 sodium channels, and 100 potassium channels, in order to generate plausible neural responses for refractory properties, like those observed in cat single-fiber experiments (Miller et al., 2001). The stochastic ion channels were implemented by the computationally efficient channel-number-tracking algorithm (Mino, et al., 2002). The other model parameters are summarized elsewhere (Matsuoka, et al., 2001). The transmembrane potentials of 2 ms in time length were generated for each simulation in which sampling steps were set at 2 μs. The transmembrane potentials were recorded at all nodes of Ranvier in the ANF model to analyze spike initiations. A stimulating electrode was located at distances of 1, 4, and 7 mm above the center node (26th) and paired masker-probe monophasic cathodic current pulses with a duration of 40 μs each were presented as stimuli. Spike occurrence time was detected by determining when the transmembrane potential took the peak amplitude and was greater than 50% of the peak amplitude of action potentials in response to masker pulses to see at which node of Ranvier the spike was initiated as well as when this occurred. A spatiotemporal histogram of spike initiations allows us to intuitively interpret distributions of spike time and initiation site.

3.3   Results

Figure 1 shows the transmembrane potentials recorded at the 36th node, $V_m(36, t)$, in response to 20 maker-probe stimulus pulses in which the MPI was varied to 1.0, 0.7, 0.5,and 0.4 ms at the electrode-to-fiber distances of 1 mm (left column), 4 mm in (middle column), and 7 mm in (right column), where the stimulus electrode was located above the 26th node. The amplitude of the masker pulse was set so that the masker can evoke spikes all times (the firing efficiency = 1.0), whreas that of the probe pulse was set so that the firing efficiency of spikes can take 0.5, i.e. threshold values. The action potential waveforms were plotted relative to the resting potential. As the MPI's were increased, the amplitude of spikes in response to probe pulses tended to decrease, whereas the temporal variation of spikes tended to increase in all cases of the electrode-to-fiber distance. When the electrode-to-fiber distance was increased, the temporal variation of spikes tended to be larger, as is seen from the results of the single pulse response shown in the seventh QPR.

Figure 2 summarizes the fundamental parameters of neural responses including Threshold in μA (top row), Latency in μs (2nd row), Jitter in μs (3rd row), and Relative Spread(RS) (bottom row) in % as a function of MPI's in which each solid line was drawn directly connecting points. The left, middle, and right columns show the fundamental parameters at the electrode-to-fiber distances of 1, 4, and 7 mm, respectively. All parameters tended to increase as the MPI shortened in all cases of the electrode-to-fiber distance. In particular, we note that the parameters of jitter and RS tended to be getting larger in which the MPI was set less than 0.5 ms. These tendency may remind us that the relative refractory properties enhance the temporal variation of spikes.

Figure 3 shows three kinds of histograms, the histogram of initiation nodes in (a), (ordinary) post-stimulus time histogram in (b), and spatio-temporal histogram of spike initiations in (c), of spikes in response to the probe pulse in which the MPI's were set at 1 (top-left), 0.7 (top-right), 0.5 (bottom-left), and 0.4 (bottom-right) ms and the electrode-to-fiber distance was set at 1 mm. We note that the histogram of initiation nodes was created by summing up the spatio-temporal histogram along a specific time axis, while the ordinary post-stimulus time histogram was generated by summing up the spatio-temporal histogram along a specific node axis. As the MPI's shortened, the histogram of initiation nodes in (a) tended to get wider,
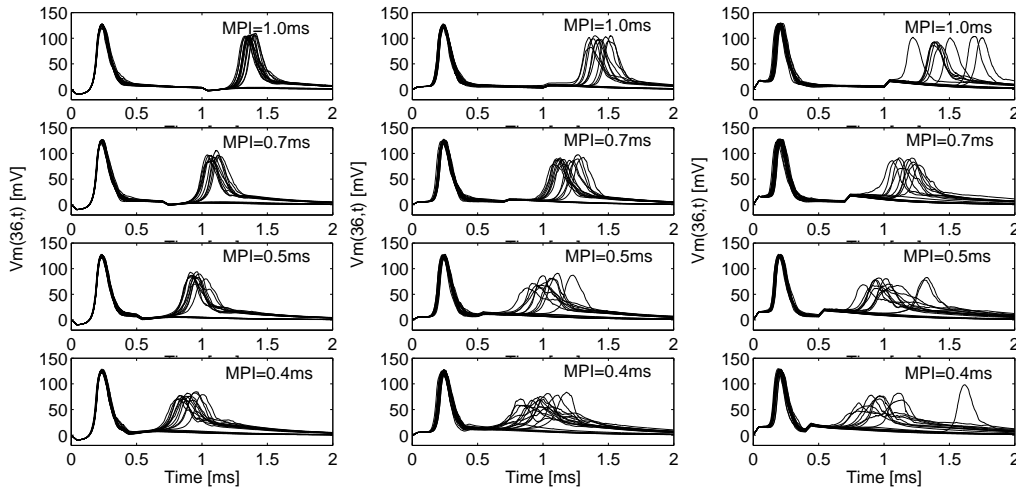
Figure 1: Action potential waveforms recorded at the 36th node of Ranvier in the ANF model as the masker-probe intervals (MPI) varied to 1.0, 0.7, 0.5 and 0.4[ms]. The left, middle, and right columns show the action potentials at the electrode-to-fiber distances of 1, 4, and 7[mm], respectively. The maker-probe stimuli were presented 20 times. The amplitude of the masker pulse was set so that the masker can evoke spikes all times (the firing efficiency = 1.0), whreas that of the probe pulse was set so that the firing efficiency of spikes can take 0.5, i.e. threshold values. The action potential waveforms were superimposed and plotted relative to the resting potential.

whereas the post-stimulus time histogram in (b) tended to become more symmetric and wider. The spatio-temporal histogram of spike initiations in (c) tells us more clearly how the spike initiations are distributed not only spatially but also temporally as the MPI's shortened. It follows from these results that the relative refractory properties enhance the variations of spike initiation sites and spiking time, making it possible to increase randomness of the underlying stochastic sodium and potassium channels as well as to generate "emergent phenomena" (Waldrop, 1992) from the interactions of the stochastic ion channels in multiple nodes of Ranvier.

Figure 4 and 5 also show three kinds of histograms of spikes in response to the probe stimulating pulse in which the masker-probe interval was set at 1 (top-left), 0.7 (top-right), 0.5 (bottom-left), and 0.4 (bottom-right) *ms* and the electrode-to-fiber distance was set 4 and 7 *mm*, respectively. These tendencies shown in Figures 4 and 5 were basically similar to those of the electrode-to-fiber of 1 *mm* shown in Figure 3. However, distributions of those histograms were found to widen as the electrode-to-fiber distance
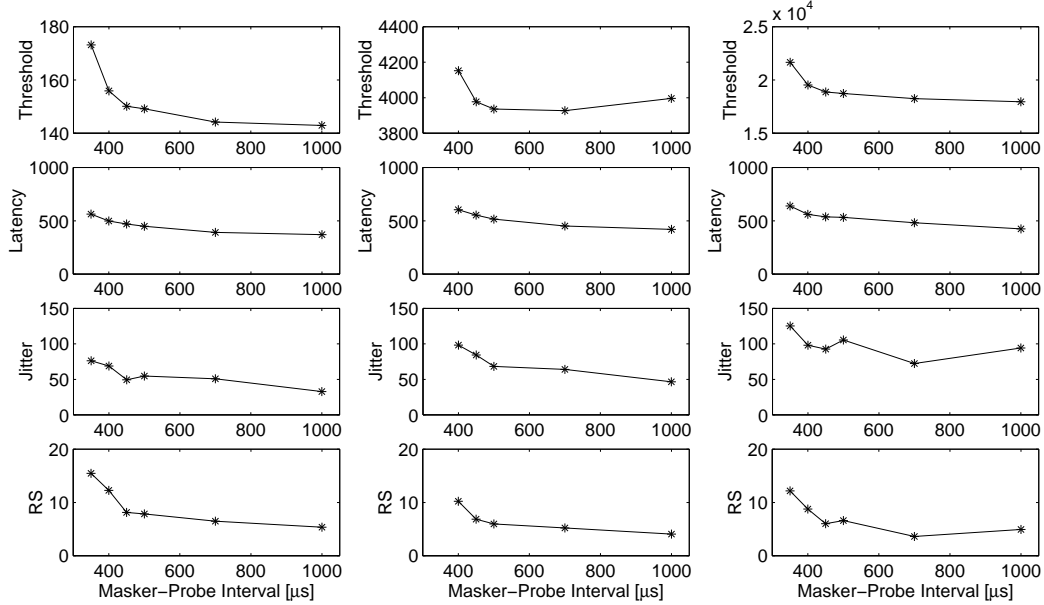
Figure 2: Fundamental parameters of neural responses, Threshold in μA (top row), Latency in μs (2nd row), Jitter in μs (3rd row), and Relative Spread(RS) (bottom row) in % as a function of MPI. The left, middle, and right columns show the parameters at the electrode-to-fiber distances of 1, 4, and 7[mm], respectively. Each solid line was drawn directly connecting points.

was increased, as is seen from the results shown in the seventh QPR. Note that as the distribution of initiation nodes becomes wider, particularly with shorter MPIs, the PST histogram becomes more symmetric like a Gaussian distribution.

3.4 Discussion

In the present QPR, we have investigated the influences of the MPI's as well as the electrode-to-fiber distance on the spatio-temporal variation of spikes in response to probe pulses under the double-pulse situation, using the ANF model. We have shown that as the MPI's shorten, the jitter and RS tend to increase and the spatio-temporal histogram of spike initiations become wider. We also have shown that as the electrode-to-fiber distance increases, the spatio-temporal distributions of spike initiations also widen, as is expected from the seventh QPR. The statistics such as jitter, RS, and distributions observed under refractory processes were greater than those in the single stimulus pulse strategy however.
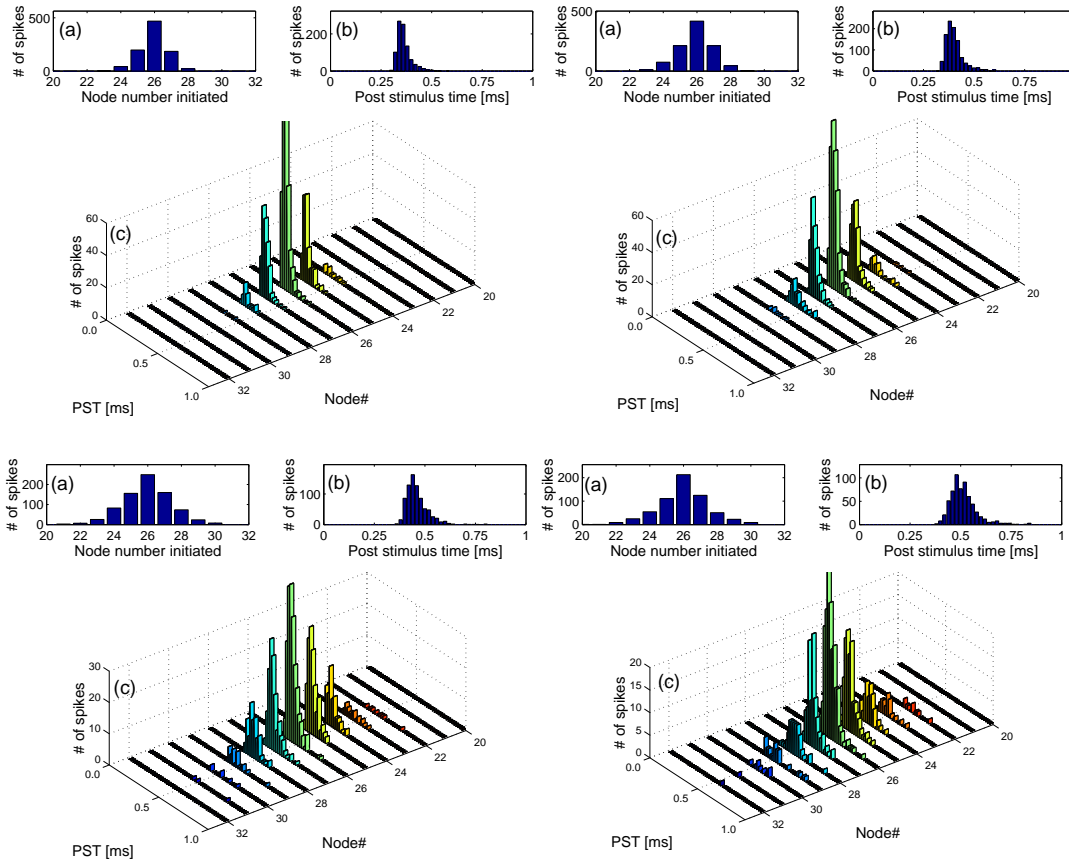
Figure 3: Statistics of the spikes in response to the probe pulse in which the masker-probe interval was set at 1 (top-left), 0.7 (top-right), 0.5 (bottom-left), and 0.4 (bottom-right) [ms] and the electrode-to-fiber distance was set at 1[mm]. (a)histogram of node initiated, (b)post-stimulus time histogram, and (c)spatio-temporal histogram of spike initiations. The masker-probe stimuli were presented 2000 times, and the probe pulse amplitude was chosen so that the firing efficiency was approximately 0.5.
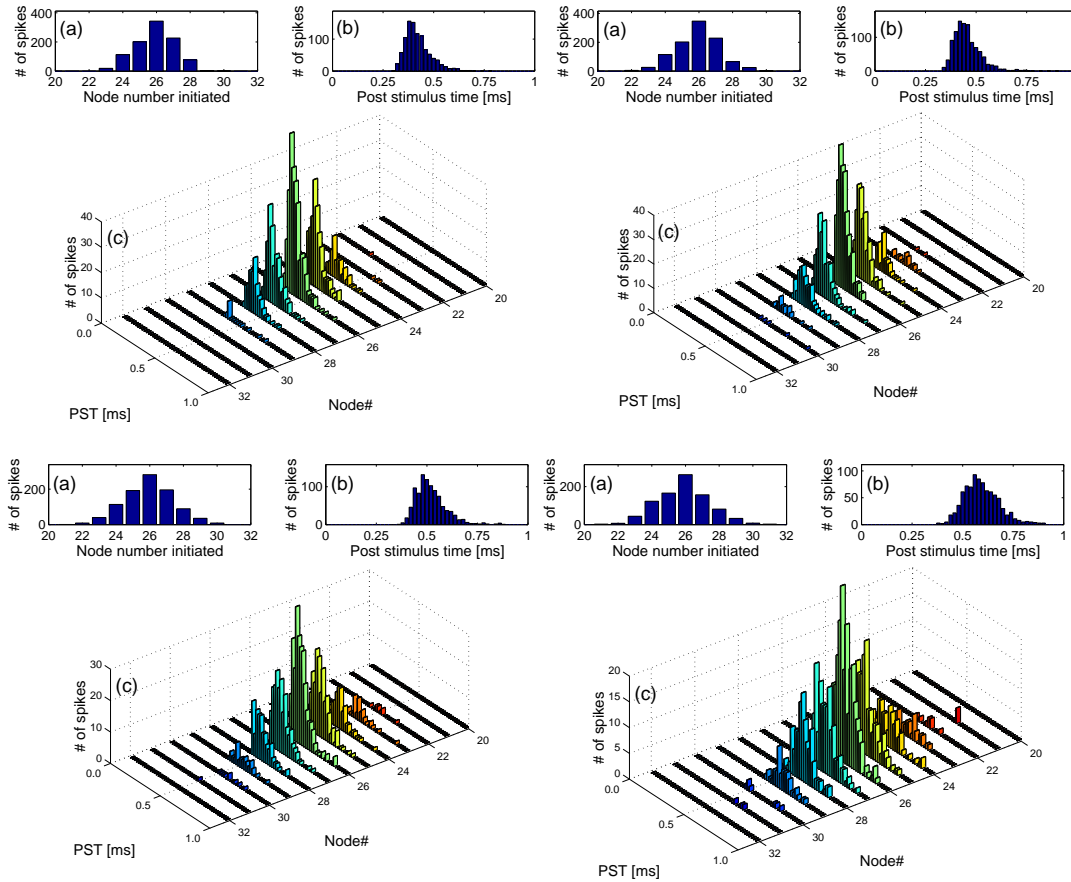
Figure 4: Statistics of the spikes in response to the probe pulse in which the masker-probe interval was set at 1 (top-left), 0.7 (top-right), 0.5 (bottom-left), and 0.4 (bottom-right) [ms] and the electrode-to-fiber distance was set at 4[mm]. (a)histogram of node initiated, (b)post-stimulus time histogram, and (c)spatio-temporal histogram of spike initiations. The masker-probe stimuli were presented 2000 times, and the probe pulse amplitude was chosen so that the firing efficiency was approximately 0.5.
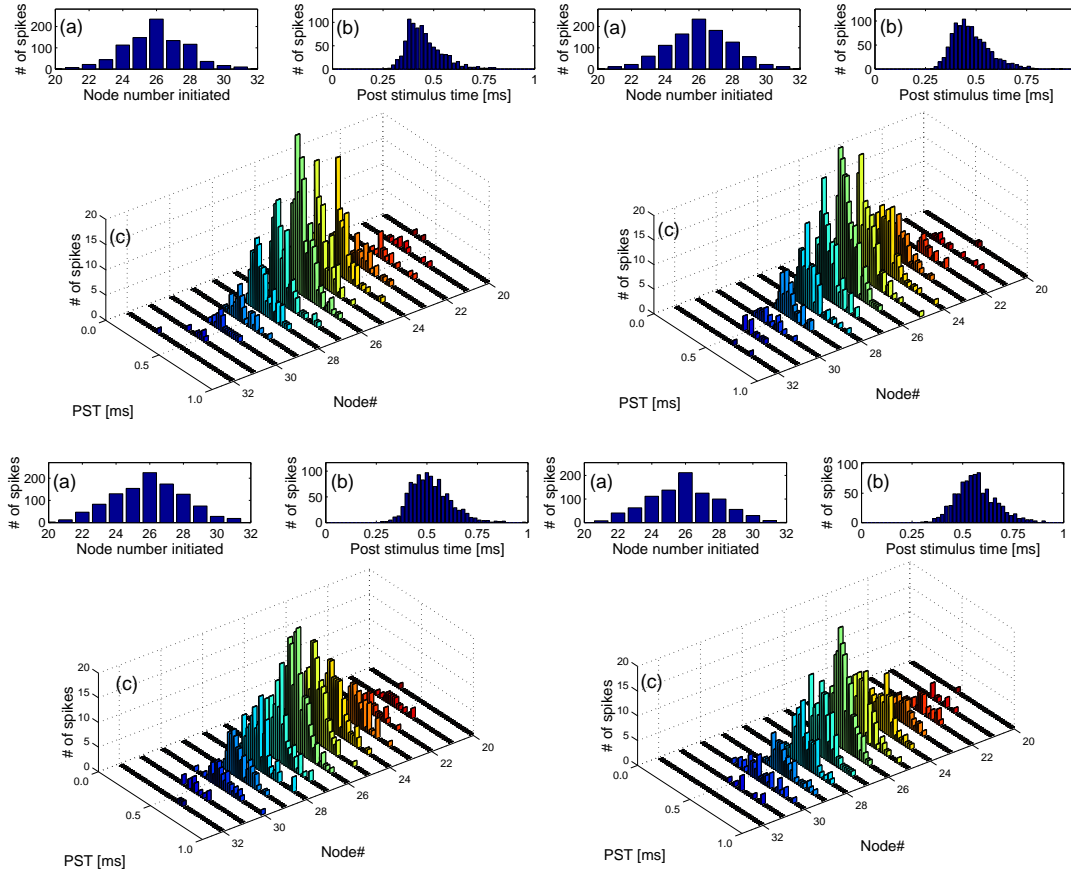
Figure 5: Statistics of the spikes in response to the probe pulse in which the masker-probe interval was set at 1 (top-left), 0.7 (top-right), 0.5 (bottom-left), and 0.4 (bottom-right) [ms] and the electrode-to-fiber distance was set at 7[mm]. (a)histogram of node initiated, (b)post-stimulus time histogram, and (c)spatio-temporal histogram of spike initiations. The masker-probe stimuli were presented 2000 times, and the probe pulse amplitude was chosen so that the firing efficiency was approximately 0.5.

These finding may imply that refractoriness enhances the randomness of spike initiations over temporal and spatial domains. That is, as the distribution of spike initiations gets wider spatially and/or temporally, the possibility of desyncronization in ANF bundles is greater. It was not expected that spatial characteristics of the stimulus field would interact so strongly with refractory properties in this manner. Even though refractoriness has been thought to limit the performance of neurons, refractory properties can be positively utilized to improve the information transfer and performance of cochlear implants, as noted by the benefit of refractoriness for neural reliability in other areas of neuroscience (Berry and Meister, 1998). In addition, the finding that as the MPI's decrease the PST histogram changes from asymmetric to symmetric may provide an experimental tool to analyze the excitation process in single-unit studies.

The computations generated with the ANF model used here were not necessarily matched perfectly to those observed in single-unit experiments. Therefore it will be necessary to continue to make efforts to match the data in computational models to those recorded in experiments (Miller et al., 1999; Miller et al., 2001). It will also be important to investigate the spatio-temporal variation of spike initiations in which spike trains are presented as stimuli. These modeling endeavors may significantly advance our understanding of information transfer in the electrically stimulated auditory nerve as well as accelerate the design of better auditory prostheses.

4   Plans for the next quarter

In the twelfth quarter, we plan to do the following:

- We will continue to collect evoked potential data on the effects of recording electrode site, with the eventual goal of aiding our interpretation of ECAP data that can be obtained from clinical subjects.

- We will analyze our ECAP data concerning adaptation to repeated (pulse-train) stimulation.

- We will collect additional data on feline single-fiber responses to stimuli delivered by different intracochlear electrode configurations.

- We will attend and present data at the 7th International Cochlear Implant Conference to be held in Manchester, England during the first week in September.

5   Appendix: Presentations and publications

The following manuscript has been published:

- Mino H, Rubinstein JT, and White JA , Comparison of Computational Algorithms for the Simulation of Action Potentials with Stochastic Sodium Channels. Annals of Biomedical Engineering, Vol.30, No.4, pp.578-587, 2002.

The following manuscripts were submitted and accepted for publication:

- Hong RS, Rubinstein JT, Wehner D, Horn D. Dynamic range enhancement for cochlear implants. Otology & Neurotology, 2002.

- Rubinstein JT, Tyler RS, Wolaver A and Brown CJ. Electrical suppression of tinnitus with high-rate pulse trains. Otology & Neurotology, 2002.

The following presentations were given:

- Dr Abbas gave an invited presentation "Electrophysiological assessment of stimulation selectivity", at the Conference on Candidacy for Implantable Hearing Devices, June 2002.

- Dr Rubinstein gave an invited presentation at the annual meeting of the American Society of Artificial Internal Organs.

References

[1] Berry, K.J. II, Meister M (1998) Refractoriness and neural precision. J. Neurosci., 18, 2200-2211.

[2] Hong, R.S, Rubinstein, J.T., Wehner, D. , Abbas, P.J., Miller, C.A. (2002) Tenth Quarterly Progress Report, N01-DC-9-2107, "The Neurophysiological Effects of Simulated Auditory Prosthesis Stimulation".

[3] Li, J., Young, E.D. (1993) Discharge-rate dependence of refractory behavior of cat auditory nerve fibers. Hear. Res., 69, 151-162.

[4] Litvak, L. (2002) Towards to a better speech processor for cochlear implants: auditory nerve responses to hi rate electric pulse trains. Ph.D. thesis, Massatusetts Institute of Technology.

[5] Matsuoka, A.J., Rubinstein, J.T., Abbas, P.J., Miller, C.A. (2001) The effects of interpulse interval on stochastic properties of electrical stimulation: models and measurements. IEEE Trans. on Biomed. Eng. 48, 416-424.

[6] Miller, C. A., Abbas, P. J., Robinson, B. K., Rubinstein, J. T., Matsuoka, A. J. (1999) Electrically evoked single-fiber action potentials from cat: responses to monopolar, monophasic stimulation. Hear. Res., 130, 197-218.

[7] Miller, C.A., Abbas, P.J, Robinson, B.K.(2001) Response properties of the refractory auditory nerve fiber. J. Assoc. Oto. Res., 02, 216-232.

[8] Mino, H., Rubinstein, J.T., Miller, C.A., Abbas, P.J. (2001) Seventh Quarterly Progress Report, N01-DC-9-2107, "The Neurophysiological Effects of Simulated Auditory Prosthesis Stimulation".

[9] Mino, H., Rubinstein, J.T., White, J.A. (2002) Comparison of Computational Algorithms for the Simulation of Action Potentials with Stochastic Sodium Channels. Annals of Biomedical Engineering, Vol.30, No.4, pp.578-587.

[10] Rubinstein, J.T., Wilson, B.S., Finley, C.C. and Abbas, P.J. (1999) Pseudospontaneous activity: stochastic independence of auditory nerve fibers with electrical stimulation. Hear. Res., 127, 108-118.

[11] Runge-Samuelson C. (2002) Response of the auditory nerve to sinusoidal electrical stimulation: effets of hi-rate pulse trains. Ph.D. thesis, The University of Iowa.

[12] Waldrop, M.M. (1992) Complexity: the Emerging Science At the Edge of Order and Chaos. Touchstone Books, New York.